14th Asia-Pacific Conference on Combustion
Kaohsiung Exhibition Center, Kaohsiung, Taiwan
14th-18th May 2023

Parametric Analysis on Ignition Assistance by a Shielded Hot Surface under Aircraft Compression Ignition Engine Conditions

Sayop Kim[1], Je Ir Ryu[1,2,4*], Austen H. Motily[3], Tonghun Lee[3], Kenneth S. Kim[4], and Chol-Bum M. Kweon[4]

[1]New York University Abu Dhabi, Abu Dhabi, UAE

[2]New York University, Brooklyn, NY, 11201, USA

[3]University of Illinois Urbana-Champaign, Urbana, IL, 61801, USA

[4]Combat Capabilities Development Command Army Research Laboratory,

Aberdeen Proving Ground, MD, 21005, USA

Abstract

This study describes optimized ignition assistance (IA) strategy regarding the parametric factors of IA devices, which supports ignition control, for aircraft compression ignition engines. Such an ignition control technique can effectively support reliable engine operation against varying altitude conditions by means of active ignition timing control. The ignition performance may vary as a function of the IA device's thermal impact and geometrical configuration and often be limited by the complex nature of the thermo-chemical process in the combustion chamber. Therefore, ultimate CI engines may require optimization of such design parameters. To this end, this study examines various parametric elements by implementing the design of experiments (DoE) analysis. The IA device with an obliquely 45-degree cut shield was used to assess the geometrical impact, and the impact of IA device temperature was added for the analysis. Total 37 numerical experiment cases were chosen for DoE input factors. The DoE analysis constructed a regression equation to express the predictive response function, which was then utilized to provide insights into ignition enhancement performance against the reference cases with bare IA devices without the shield design.

1 Introduction

Compression ignition (CI) engines exhibit the ability to improve fuel efficiency and low CO_2 emissions in numerous land-based vehicle powertrain systems. Such benefits may apply equivalently to practical aircraft propulsion systems. However, variable altitude conditions for aircraft engines may extremely challenge engineers to secure reliable ignition control. Especially at high altitude conditions, the CI engine may encounter issues of ignition failure and incomplete combustion [1]. In addition, variability in fuel properties and quality between land-based engines and aircraft engines may hold difficulties associated with the co-optimization of fuel and engines. Of many technical challenges, ignition control is regarded as an essential technique and many literatures have been dedicated to discovering ignition assistance (IA) techniques. For land-based vehicle CI engines, mixing controlled ignition assistance was examined for CI engines by implementing a pilot injection strategy, and hence local reactivity control was made possible [2]. Local thermal energy deposit is widely used to promote ignition in diesel engines, and they employ a glow plug system, called ignition assistance (IA) device hereafter [3, 4]. Several experiments were recently carried out to demonstrate the possibility of the IA device's hot surface assisted ignition enhancement by using an optical engine [5, 6, 7]. Extended numerical studies were also attempted to discover the importance of IA device surface temperature and design factors associated with F-24 aviation jet fuel [8, 9].

In this study, the geometrical configuration of the IA device was highlighted in the analysis with an emphasis on the heating element shield design. The conventional bare IA device was originally developed to assist engine cold starts for land-based diesel engines. However, the IA device may constantly operate for high-altitude aircraft engines and thus it is vulnerable to the constant thermo-mechanical stress build-up without the proper shield protection [10, 11]. In addition, the shield may partially cover the hot surface and thereby prevent thermal loss possibly caused by a cool intake air [12]. It helps to partially trap the fuel-air mixture within the thermal boundary layer and thus promote ignition adjacent to the hot surface. On the other hand, the well-shielded IA device may inversely act in a way that it delays the ignition due to its intrinsic cold surface [13]. Such a simultaneous conflicting effect has not been thoroughly understood to this date. To simultaneously maximize the ignition enhancement and secure the system durability, geometrical and operational IA device optimization is needed. Towards this aim, in this paper, numerical experiments that performed the design of experiments (DoE) are presented to further discuss the effect of IA device surface temperature in conjunction with several geometrical dimensions in an obliquely cut shield. Direct injection F-24 jet fuel was used in the analysis and high-altitude relevant operating conditions were employed. Thus, this study aims to discuss the dominant design factors and their optimization for aircraft CI engines.

2 Numerical Simulation Setup and Design of Experiment

For the present analysis, the initial and boundary conditions, the geometry of the combustion chamber, and injector parameters were based on the rapid compression machine (RCM) setup described in the previous literatures [8, 13]. Three-dimensional CFD simulations were conducted with the vertically injecting jet

---

*Corresponding author
E-mail address: jryu@nyu.edu

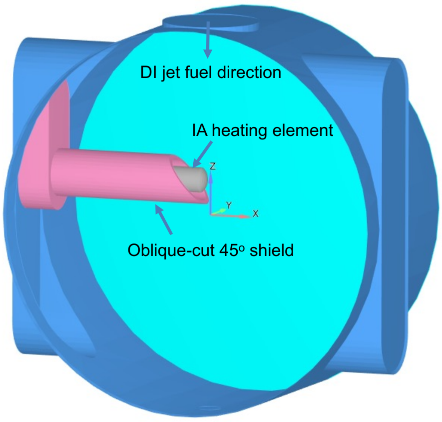

Figure 1: The CFD domain represents the RCM chamber setup. IA device and DI F-24 fuel injection were employed.

Table 1. Selected DoE design variables

Gap size [mm]	0.5, 1.0, 1.5
Relative position [-]	-1, -0.5, 0, 0.5, 1
IA tip location [mm]	-1, -0.5, 0, 0.5, 1
IA temperature [K]	1200, 1300, 1400, 1500, 1600

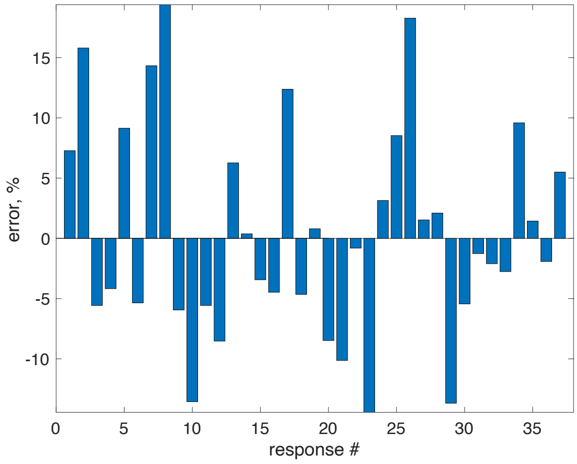

Figure 2: Predictive accuracy obtained from the predictive regression equation based on ignition delay.

fuel and the horizontally mounted IA device with the obliquely cut 45° shield in the chamber domain as displayed in Figure 1. The modeled IA device used in this study adopted a commercially available Bosch Duraspeed glow plug as a hot surface probe with a tip radius of 2 mm. The heating element of the IA device was modeled by adopting the constant temperature heating core model [8]. The initial/boundary conditions were set to 800 K of ambient air temperature and wall temperature, 3 MPa of chamber pressure, and 400 K of intact fuel temperature. The injector orifice diameter was 147 µm and injected mass was 7.6 mg. Details of the setup can be found in the previous study [8].

For transient compressible reacting flow simulations, CONVERGE CFD solver was used. A fixed embedding grid refinement was implemented around the spray plume and the IA device component. A multi-level adaptive mesh refinement was applied to account for transient and small-scale turbulent mixing and reactive scalars, thereby the minimum grid size yielded 0.125 mm. Eulerian-Lagrangian (EL) method was used to model the liquid spray injection and their atomization/evaporation process. For chemical reactions, a recently developed data-driven mechanism [14] was used to better represent underlying reaction steps and chemical species of the employed F-24 fuel.

To facilitate the DoE analysis, four IA design factors were selected such as gap, relative position, tip location, and IA temperature. The gap is a gap between the heating element and the shield. The relative position suggests the location of the shield end-tip with respect to the heating element end-tip. Tip location defines the horizontal location of the end-tip of the IA device with respect to the spray axis ($x = 0$). Meanwhile, in this setup, the vertical location of the IA device was fixed at 21 mm downstream of the injector location, which is equivalent to the average liquid penetrating length of the F-24 fuel given the test condition. Tested variations of each parametric factor are listed in Table 1. Using the optimal Latin hypercube sampling based on the selected 4 factors, total 37 cases were chosen for the numerical experiments instead of running all possible cases.

The DoE analysis was conducted based on the DoE response, which was determined by the pressure recovery ignition delay. The ignition delay was obtained from the time when the pressure recovers to the value without the injection [15]. From the simulation results, a predictive equation, which is polynomial regression, was constructed as a function of chosen DoE design factors. The reproduced ignition delay from the predictive equation was compared against the CFD results and showed a moderate range of errors as shown in Figure 2. The error may have arisen due to the lack of sampling size. Equivalent details of DoE technique can be found in the previous literature [16].

Other than the chosen DoE cases, additional reference cases were also conducted. One simulation was set up without the IA device and several other simulations were dedicated to running the cases with the bare IA device without a shield installed. These reference cases can provide baseline conditions to assess the impact of chosen IA device configurations.

3 Results

3.1 Impact of IA device

Figure 3 shows the results from the simulation with the bare IA device. This demonstrates the advanced ignition performance by means of a local thermal-energy deposit. Compared to the free spray case (w/o IA), all tested cases were found to ignite much earlier than 2.4 ms of the free spray. Details of ignition performance may vary depending on the IA device configuration. In general, the most noticeable ignition delay difference can be found across the IA device temperature change. IA device design

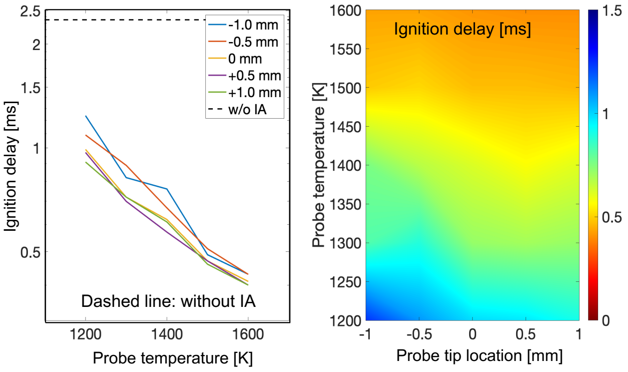

Figure 3. Improved ignition performance by means of IA device

factors can also affect the ignition performance, i.e., shifted tip location towards spray axis (increased *x*) caused fast onset of ignition. This is because increased physical impact between the spray plume and IA device helps to increase the local fuel-air mixture reactivity.

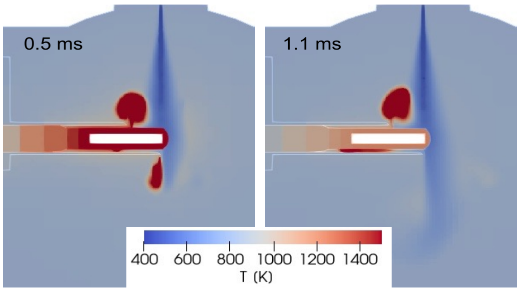

Figure 4. Ignition pocket formation with different IA device temperatures: 1600 K (left) and 1200 K (right)

Figure 4 illustrates the ignition pocket formation with the IA device covered by the shield. Due to the local thermal energy deposit at the impact point, the ignition pocket starts to grow from the heating element surface. The secondary ignition pocket attached to the IA device tip can be developed downstream along with the spray plume edge at 1600 K condition. This is because of the reduced ignition delay at the high IA device temperature and thereby typical spray combustion starts to grow as reported in the previous literature [8].

As stated earlier, the shield can play a role in trapping the spray mixture around the hot IA device surface and thus possibly increase local chemical reactivity, resulting in a shorter ignition delay. It is also inversely possible that the shield may delay the ignition due to the elongated mixing residence time of the trapped mixture along with possible heat loss at the cold shield surface. In addition, the mix of elongated mixing residence time and the presence of gap design may be a reason for rich mixture build-up off the flammability limit. To further discover such a contradictory effect, Figure 5 shows the effects of input factors on ignition delay. The solid line follows the overall propensity (average) ignition delay over the chosen input factor. The dashed line represents the upper and lower bounds over the DoE cases.

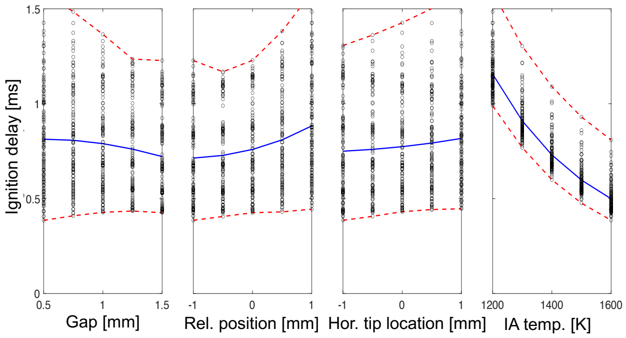

Figure 5. Effects of DoE design factor on ignition delay. Blue solid line: average, red dashed lines: upper/lower bounds.

Increased gap size tends to make fuel-air mixture ignite more rapidly. However, the upper bound and lower bound show the opposite trend and this implies that dominance of the gap size impact may be taken over by the other design factors or the complex nature of the turbulent mixing process. Contrary to the gap size test, increased relative position and horizontal tip location delay the average ignition. For the relative position test, the non-linear upper bound trend can be indicative of another complexity of the design factor and the abovementioned contradictory effect. It is interesting to note that the current increased horizontal tip location test presents the opposite trend from the previous bare IA device test in Figure 3. It is possible that the presence of a shield gap may hinder the sequential

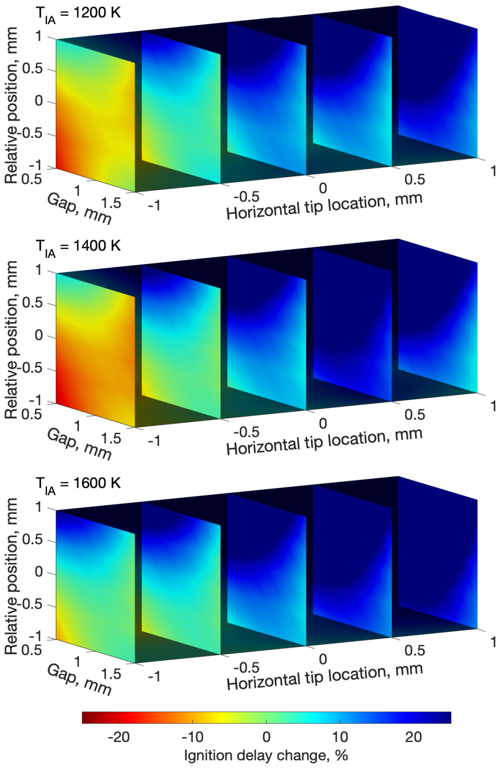

(a) Relative ignition delay improvement

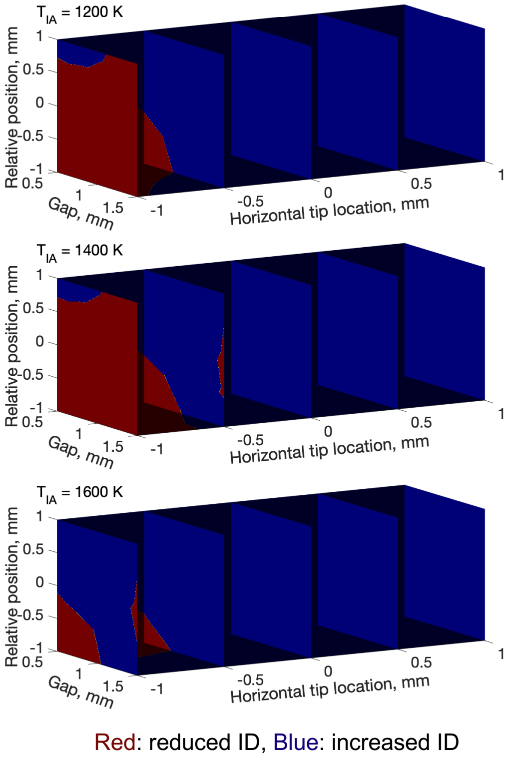

(b) Ignition improvement identifier

Figure 6. Ignition delay improvement compared to reference cases (w/o IA device shield)

combustion process from the rich mixture within the thermal boundary layer due to potential thermal energy loss at the cold shield surface.

In general, however, the increased surface temperature dramatically drops the ignition delay time and thus becomes the most dominant factor from the current DoE analysis. Although their geometric design impact is marginal compared to the IA device temperature, more broadly ranged sampling cases can potentially discover the relationship between different design factors.

Figure 6 (a) depicts a comprehensive color map of ignition delay change over the employed DoE design factors with respect to the values of reference cases. Here, the reference cases were cast as bare IA setups without the shield installed. Figure 6 (b) identifies the limited region of ignition enhancement by the shield design, e.g., the red color map representative of the advanced ignition regime. Such an enhancement became very minimal or was taken over by the worse ignition performance.

From the results, the contradictory effect, delayed ignition by the shield, is clearly seen. The effect of the IA device shield on the ignition became relatively positive as the IA device temperature decreases by identifying the larger area of reduced ignition delay at 1200 K case (e.g., red color map). However, under high IA device temperature conditions, ignition enhancement is barely found, rather they increase the ignition delay time and show worse performance. This suggests that tested input factor ranges did not completely overcome the contradictory effect resulting in delayed ignition possibly due to the heat loss to the shield surface. However, the potential ignition enhancement was demonstrated at the low IA device temperature condition, meaning that optimal design for the high-temperature condition may put forth better results. To secure the benefit of the system durability such as IA heating element protection, the use of a shield is desired, and therefore thoroughly optimized shielded IA device configuration is required.

4 Conclusions

Numerical simulations and DoE analysis of F-24 jet fuel injected into a combustion chamber with an IA device were performed to investigate the effect of several IA design input factors on ignition delay. From the results addressed above, the following conclusions can be summarized:

- The IA device can effectively assist ignition in the chamber by elevating the local thermal energy and promote autoignition. This improvement was found more effective as the IA device temperature increases.
- During the assisted ignition process, isolated ignition pocket forms near the IA device hot surface. Also, a secondary ignition pocket can be separately developed at further increased IA device temperature.
- The employed obliquely cut shield design may or may not support the ignition enhancement depending on the detailed design configuration of gap size, relative tip position, and horizontal tip location due to a possible contradictory effect, which causes a worse ignition performance despite the shield.
- The contradictory effect is possibly caused by a mix of local thermal energy loss at the cold shield surface and the off-flammability limit trend that essentially becomes clear when the rich mixture deposit becomes heavy near the gap between the shield and the IA device surface.
- Despite the reported contradictory effect, potential of shield in the IA device was demonstrated at low IA device temperature. Thoroughly optimized shield design can possibly provide extended coverage of ignition enhancement for high temperature IA device.

5 Acknowledgment

This work was supported by an annual research grant provided by New York University Abu Dhabi. Research was also sponsored by the Army Research Laboratory and was accomplished under Cooperative Agreement Number W911NF-18-2-0282 while J.I.R. was a postdoctoral fellow at the Army Research Laboratory. The views and conclusions contained in this document are those of the authors and should not be interpreted as representing the official policies, either expressed or implied, of the Army Research Laboratory or the U.S. Government. The U.S. Government is authorized to reproduce and distribute reprints for Government purposes notwithstanding any copyright notation herein.

References

[1] K. S. Kim, M. T. Szedlmayer, C.-B. M. Kweon, K. K. M., J. A. Gibson, C. A. Lindsey, R. D. Meininger, M. R. Musser and A. V. Giddings, 53rd AIAA/SAE/ASEE Joint Propulsion Conference, 2017.

[2] R. Rajasegar, Y. Niki, Z. Li, J. M. Garcia-Oliver and M. P. B. Musculus, Proceedings of the Combustion Institute, vol. 38, pp. 5741-5750, 2021.

[3] A. Ramesh, B. Nagalingam and K. V. Gopalakrishnan, SAE Technical Paper, vol. 921632, 1992.

[4] C. J. Mueller and M. P. Musculus, SAE Technical Paper 2001-01-20, 2001.

[5] E. R. Amezcua, D. A. Rothamer, K. S. Kim and C.-B. M. Kweon, AIAA SciTech Forum, 2020.

[6] E. R. Amezcua, K. Kim, D. Rothamer and C.-B. Kweon, SAE Int. J. Advances & Curr. Prac. in Mobility, vol. 4, no. 5, pp. 1651-1666, 2022.

[7] N. Miganakallu, J. Stafford, E. Amezcua, K. S. Kim, C.-B. M. Kweon and D. A. Rothamer, Proceedings of the ASME, ICEF2022-90704, 2022.

[8] J. I. Ryu, A. H. Motily, R. Scarcelli, S. Som, K. S. Kim, C.-B. M. Kweon and T. Lee, AIAA SciTech 2020 Forum, 2020.

[9] H. D. Sapra, R. P. Hessel, E. R. Amezcua, J. Stafford, N. Miganakallu, D. Rothamer, K. Kim, C. M. Kweon and S. Kokjohn, Proceedings of the ASME, ICEF2022-89329, 2022.

[10] S. G. Kang, J. I. Ryu, A. H. Motily, P. Numkiatsakul, T. Lee, W. M. Kriven, K. S. Kim and C.-B. M. Kweon, Journal of Propulsion and Power, vol. 38, no. 4, 2022.

[11] S. G. Kang, J. I. Ryu, A. H. Motily, P. Numkiatsakul, T. Lee, W. Kriven, K. S. Kim, and C.-B. M. Kweon, AIAA Propulsion and Energy 2021 Forum, AIAA 2021-3615, 2021.

[12] J. Lorusso and H. Cikanek, SAE Technical Paper 880495, 1988.

[13] A. H. Motily, E. Wood, T. Lee, J. I. Ryu, K. S. Kim and C.-B. M. Kweon, AIAA SciTech Forum (Virtual), 2021.

[14] J. I. Ryu, K. Kim, R. Scarcelli, S. Som, K. S. Kim, J. E. Temme, C.-B. M. Kweon and T. Lee, Fuel, vol. 290, p. 119508, 2021.

[15] K. Miwa, T. Ohmija and T. Nishitani, JSME International Journal, vol. 31, no. 1, pp. 166-173, 1988.

[16] J. I. Ryu, A. H. Motily, T. Lee, R. Scarcelli, S. Som, K. S. Kim and C.-B. M. Kweon, 2020 AIAA Propulsion and Energy Forum, 2020.